

# Can anisotropy in the galaxy distribution tell the bias?

Biswajit Pandey<sup>\*</sup>

*Department of Physics, Visva-Bharati University, Santiniketan, Birbhum, 731235, India*

9 October 2018

## ABSTRACT

We use information entropy to analyze the anisotropy in the mock galaxy catalogues from dark matter distribution and simulated biased galaxy distributions from  $\Lambda$ CDM N-body simulation. We show that one can recover the linear bias parameter of the simulated galaxy distributions by comparing the radial, polar and azimuthal anisotropies in the simulated galaxy distributions with that from the dark matter distribution. This method for determination of the linear bias requires only  $O(N)$  operations as compared to  $O(N^2)$  or at least  $O(N \log N)$  operations required for the methods based on the two-point correlation function and the power spectrum. We apply this method to determine the linear bias parameter for the galaxies in the 2MASS Redshift Survey (2MRS) and find that the 2MRS galaxies in the  $K_s$  band have a linear bias of  $\sim 1.3$ .

**Key words:** methods: numerical - galaxies: statistics - cosmology: theory - large scale structure of the Universe.

## 1 INTRODUCTION

The homogeneity and isotropy of the Universe on large scales is a fundamental tenet of modern cosmology. Our current understanding of the cosmos relies heavily on this principle. Presently a large number of cosmological observations such as the temperature of the Cosmic Microwave Background (CMBR) (Smoot et al. 1992; Fixsen et al. 1996), X-ray background (Wu et al. 1999; Scharf et al. 2000), angular distributions of radio sources (Wilson & Penzias 1967; Blake & Wall 2002), Gamma-ray bursts (Meegan et al. 1992; Briggs et al. 1996), supernovae (Gupta & Saini 2010; Lin et al. 2016), galaxies (Marinoni et al. 2012; Alonso et al. 2015) and neutral hydrogen (Hazra & Shafieloo 2015) are known to favour the assumption of statistical isotropy. But this assumption does not hold on small scales and the anisotropies present on these scales can tell us a lot about the Universe. For example, the CMBR is not completely isotropic and the anisotropies imprinted in the CMBR perhaps provide the richest source of information in cosmology (Planck Collaboration et al. 2016). In the current paradigm, the large scale structures in the Universe are believed to emerge from the gravitational amplification of the miniscule density fluctuations generated in the early Universe. The anisotropies in the CMBR shed light on the conditions that prevailed in the early Universe whereas the anisotropies in the present day mass distribution help us to unravel the

formation and evolution of the large scale structures in the Universe.

Currently there exist a wide variety of statistical tools to quantify the distribution of matter in the Universe. Besides their use in the study of CMBR anisotropies, the two-point correlation function and the power spectrum also remain the most popular choice for the study of clustering. The two-point correlation function (Peebles 1980) measures the amplitude of galaxy clustering as a function of scale whereas the shape and amplitude of the power spectrum also provide the information about the amount and nature of matter in the Universe. The three-point correlation function and the bispectrum has been also widely used in the study of clustering in the galaxy distribution. These statistics are popular as one can directly relate them to the theories of structure formation.

The distribution of galaxies are believed to trace the mass distribution on large scales, where the density fluctuations in galaxies and mass are assumed to be related linearly (Kaiser 1984; Dekel & Rees 1987). In the linear bias assumption, both the two point correlation function and power spectrum can be employed to determine the linear bias between galaxies and mass (Norberg et al. 2001; Tegmark et al. 2004; Zehavi et al. 2011). The distribution of the galaxies are inferred from their redshifts. The peculiar velocities induced by the density fluctuations perturb their redshifts. This distorts the clustering pattern of galaxies in redshift space and cause the two-point correlation function and power spectrum to be anisotropic. They are suppressed

<sup>\*</sup> E-mail: biswap@visva-bharati.ac.in

on small scales due to the motion of galaxies inside virialized structures and enhanced on large scales due to coherent flows into over dense regions and out of under dense regions. The anisotropies in the two-point correlation function and the power spectrum can be decomposed into different angular moments (Kaiser 1987; Hamilton 1992) and their ratios can be used to determine the linear distortion parameter  $\beta \approx \frac{\Omega_m^{0.6}}{b}$  where  $\Omega_m$  is the mass density parameter and  $b$  is the linear bias parameter. This method has been used to determine the linear bias (Hawkins et al. 2003; Tegmark et al. 2004). One can also use the three-point correlation function and bispectrum (Feldman et al. 2001; Verde et al. 2002; Gaztañaga et al. 2005) to measure the bias. It may be noted that some sort of parameter degeneracies are involved in all these methods. Computing the correlation functions and the poly spectra are also computationally expensive for very large data sets.

The information entropy is related to the higher order moments of a distribution and hence captures more information about the distribution. Pandey (2016b) propose a method based on the information entropy-mass variance relation to determine the large scale linear bias from galaxy redshift surveys. We investigate if this relation also holds for the anisotropy measure proposed in Pandey (2016a) and can one exploit this relation to measure the linear bias by directly measuring the anisotropy in the galaxy distribution. An important advantage of this method is the fact that for any given data set, it is computationally less expensive than the methods which are based on the two-point correlation function and the power spectrum. The only disadvantage of the method is that the information entropy is sensitive to binning and sampling. But this relative character of entropy does not pose any problem provided the distributions are compared with the same binning and sampling rate.

The modern redshift surveys (SDSS, York et al. 2000; 2dFGRS, Colles et al. 2001; 2MRS, Huchra et al. 2012) have now mapped the galaxy distribution in the local Universe with unprecedented accuracy. The SDSS and 2dFGRS are deeper than 2MRS but they only cover parts of the sky. Moreover the 2MASS redshift survey (2MRS) maps the galaxies over nearly the entire sky ( $\sim 91\%$ ) out to a distance of 300 Mpc. Unlike its optical counterparts, the 2MRS selects galaxies in the near infrared wavelengths around  $2\mu m$  which makes it less susceptible to extinction and stellar confusion. The old stellar populations which are otherwise missed by the optical surveys are also retained in 2MRS due to its operation in the infrared window. The survey is 97% complete down to the limiting magnitude of  $K_s = 11.75$  which provides a fair representation of the mass distribution in the local Universe. These advantages offered by the 2MRS over the other surveys make it most suitable for the analysis in the present work.

We use a  $\Lambda$ CDM model with  $\Omega_{m0} = 0.31$ ,  $\Omega_{\Lambda 0} = 0.69$  and  $h = 1$  for converting redshifts to distances throughout our analysis.

A brief outline of the paper follows. In section 2 we describe the method of analysis followed by a description of the data in section 3. We present the results and conclusions in section 4.

## 2 METHOD OF ANALYSIS

The information entropy was first introduced by Claude Shannon (Shannon 1948) to find the most efficient way to transmit information through a noisy communication channel. It quantifies the uncertainty in the measurement of a random variable. Given a probabilistic process with probability distribution  $p(x)$  where the random variable  $x$  has  $n$  outcomes given by  $\{x_i : i = 1, \dots, n\}$ , the average amount of information to describe the random variable  $x$  is given by,

$$H(x) = - \sum_{i=1}^n p(x_i) \log p(x_i) \quad (1)$$

The quantity  $H(x)$  is known as the information entropy of the random variable  $x$ .

Pandey (2016a) propose an anisotropy measure based on the information entropy and carry out tests on various isotropic and anisotropic distributions to find that it can efficiently recover various types of anisotropies inputted in a distribution. The method divides the entire sky into equal area pixels by carrying out uniform binning of  $\cos \theta$  and  $\phi$ . Here  $\theta$  and  $\phi$  are respectively the polar and azimuthal angles in spherical polar co-ordinates. The entire sky is divided into  $m_{total} = m_\theta m_\phi$  angular bins or pixels where  $m_\theta$  and  $m_\phi$  correspond to the number of bins used for binning  $\cos \theta$  and  $\phi$  respectively. At any distance  $r$ , each of these pixels subtend equal volumes. The method counts the number of galaxies inside each of these volume elements and define a random variable  $X_{\theta\phi}$  with  $m_{total}$  outcomes each given by,  $f_i = \frac{n_i(<r)}{\sum_{i=1}^{m_{total}} n_i(<r)}$ . The  $f_i$  represents the probability of finding a randomly selected galaxy in the  $i^{th}$  bin and we have  $\sum_{i=1}^{m_{total}} f_i = 1$ .

One can write the information entropy associated with  $X_{\theta\phi}$  for a given  $r$  as,

$$\begin{aligned} H_{\theta\phi}(r) &= - \sum_{i=1}^{m_{total}} f_i \log f_i \\ &= \log N - \frac{\sum_{i=1}^{m_{total}} n_i(<r) \log n_i(<r)}{N} \end{aligned} \quad (2)$$

where  $N$  is the total number of galaxies which are distributed within a distance  $r$  across all the bins. The base of the logarithm can be chosen arbitrarily and we choose it to be 10 for the present work.

The information entropy  $H_{\theta\phi}$  will have the maximum value  $(H_{\theta\phi})_{max} = \log m_{total}$  for a given choice of  $m_\theta$ ,  $m_\phi$  and  $r$  when the probability  $f_i$  becomes  $\frac{1}{m_{total}}$  and identical for all the bins. The anisotropy parameter  $a_{\theta\phi}(r)$  is defined as  $a_{\theta\phi}(r) = 1 - \frac{H_{\theta\phi}(r)}{(H_{\theta\phi})_{max}}$ . Ideally an isotropic distribution will always have maximum entropy and consequently  $a_{\theta\phi}(r)$  will be zero. The value of  $a_{\theta\phi}(r)$  thus characterizes the degree of anisotropy present in a distribution. It may be noted that a discrete isotropic distribution will always show a small but non-zero value for  $a_{\theta\phi}(r)$  due to shot noise. In other words, the measure is sensitive to binning and sampling and one should always compare the degree of anisotropy in two different distributions with same binning and sampling rate.

Besides characterizing the radial anisotropy  $a_{\theta\phi}(r)$ , one can also quantify the polar and azimuthal anisotropies by measuring  $a_\phi(\theta) = 1 - \frac{H_\phi}{(H_\phi)_{max}}$  and  $a_\theta(\phi) = 1 - \frac{H_\theta}{(H_\theta)_{max}}$  respectively. This would require to carry out the sum in

Equation 2 respectively over  $m_\phi$  or  $m_\theta$  bins instead of  $m_{total}$ . We fix the radius to a value  $r_{max}$  in this case. The number  $N$  in these cases would be the total number of galaxies residing in the  $m_\phi$  or  $m_\theta$  bins available at different  $\theta$  or  $\phi$  respectively.

One can write the number counts as  $n_i(< r) = n_0(< r) + \delta n_i(< r)$  where  $\delta n_i(< r)$  are small fluctuations around the mean  $n_0(< r)$  and express the entropy deficit  $(H_{\theta\phi})_{max} - H_{\theta\phi}(r)$  in terms of the different moments of the distribution (Pandey 2016b) as,

$$(H_{\theta\phi})_{max} - H_{\theta\phi}(r) = \frac{1}{2 m_{total} n_0(< r)^2} \sum_{i=1}^{m_{total}} \delta n_i^2(< r) - \frac{1}{6 m_{total} n_0(< r)^3} \sum_{i=1}^{m_{total}} \delta n_i^3(< r) + \frac{1}{3 m_{total} n_0(< r)^4} \sum_{i=1}^{m_{total}} \delta n_i^4(< r) - \dots \quad (3)$$

The first term in the above expression can be clearly identified with the variance  $\sigma_r^2$  in the number counts. Neglecting the contributions from the higher order moments in the limit  $\frac{\delta n_i(< r)}{n_0(< r)} \ll 1$ , one can relate the entropy deficit to the variance in number counts as,

$$(H_{\theta\phi})_{max} - H_{\theta\phi}(r) = \frac{\sigma_r^2}{2} \quad (4)$$

One may note that if the particles or galaxies are assumed to have equal masses then this variance in the number counts can be treated as the mass variance in those volume elements. The cosmological mass variance of a smoothed density field can be also determined from the power spectrum as,

$$\sigma_r^2 = \frac{1}{(2\pi)^2} \int_0^\infty k^2 P(k) \widetilde{W}^2(kr) dk \quad (5)$$

where,  $r$  is the size of the filter used for smoothing,  $P(k)$  is the power spectrum and  $\widetilde{W}(kr)$  is the Fourier transform of the filter. The filter shape has to be specified which would then determine  $\widetilde{W}(kr)$ . We carry out our analysis in co-ordinate space where averaging kernels have exactly same volume but somewhat different shapes. We do not expect this small variation in the shapes to make a difference when the kernels have larger volumes.

One can then use the entropy deficit  $(H_{\theta\phi})_{max} - H_{\theta\phi}(r)$  of a distribution to determine its linear bias on large scales where the density fluctuations are smaller. On large scales,  $P_g(k) = b^2 P_m(k)$  and consequently the linear bias is given by,

$$b = \sqrt{\frac{[(H_{\theta\phi})_{max} - H_{\theta\phi}(r)]_g}{[(H_{\theta\phi})_{max} - H_{\theta\phi}(r)]_m}} = \sqrt{\frac{[a_{\theta\phi}(r)]_g}{[a_{\theta\phi}(r)]_m}} \quad (6)$$

where the subscripts  $g$  and  $m$  corresponds to galaxy and mass respectively.

The same argument also holds for the polar and azimuthal anisotropies and one can use them independently to measure the linear bias for a given galaxy distribution. We do not expect them to be different and it would be interesting to measure and compare them. We analyze the anisotropies in the galaxy distribution from the 2MRS following the method outlined in this section and determine the linear bias parameter.

It may be noted that one can use any spherical coordinates for this analysis. In the present work, we use the galactic co-ordinates  $(l, b)$ . Accordingly we replace  $\theta$  and  $\phi$  in the previous definitions by  $b$  and  $l$  respectively.

### 3 DATA

#### 3.1 2MRS CATALOGUE

The Two Micron All Sky Redshift Survey (2MRS) (Huchra et al. 2012) is an all-sky redshift survey in the near infra-red wavelengths. The survey is 97.6% complete to a limiting magnitude of  $K_s = 11.75$  and covers 91% of the sky. It provides the spectroscopic redshifts of  $\sim 45,000$  galaxies in the nearby Universe. 2MRS selects the galaxies with apparent infrared magnitude  $K_s \leq 11.75$  and colour excess  $E(B - V) \leq 1$  in the region  $|b| \geq 5^\circ$  for  $30^\circ \leq l \leq 330^\circ$  and  $|b| \geq 8^\circ$  otherwise. Huchra et al. (2012) rejected the sources which are of galactic origin (multiple stars, planetary nebulae, HII regions) and discarded the sources which are in regions of high stellar density and absorption. The final 2MRS catalog by Huchra et al. (2012) contain 43,533 galaxies. We restrict our sample to  $z \leq 0.12$  beyond which there are a very few galaxies. This redshift limit is used to simulate the mock catalogues for the 2MRS. We use this 2MRS flux limited sample which contains 43,305 galaxies.

To construct mock catalogues for the 2MRS flux limited sample we first model the redshift distribution using a parametrized fit (Erdoğdu et al. 2006a,b) given by,

$$\frac{dN(z)}{dz} = A z^\gamma \exp\left[-\left(\frac{z}{z_c}\right)^\alpha\right] \quad (7)$$

We calculate the redshift distribution in the 2MRS using uniform bin size of  $200 \text{ km/s}$  and then fit it with Equation 7 using the nonlinear least-squares method (Marquardt-Levenberg algorithm). Each point in the data are assigned equal weights. We find the values of the best fit parameters to be  $A = 116000 \pm 5100$ ,  $\gamma = 1.188 \pm 0.093$ ,  $z_c = 0.031 \pm 0.002$  and  $\alpha = 2.059 \pm 0.149$ . The redshift histogram in the 2MRS along with the best fit (Equation 7) curve is shown in the left panel of Figure 1. It may be noted that dividing Equation 7 by the total number of galaxies gives the probability of detecting a galaxy at redshift  $z$ .

We would like to have a galaxy distribution over full-sky for our analysis. This requires us to artificially fill the Zone of Avoidance (ZOA), the region near the Galactic plane which is obscured due to the extinction by Galactic dust and stellar confusion. We randomly select galaxies from the unmasked region and then place them at random locations in the masked area so as to have the same average density in the masked and unmasked region (Lynden-Bell et al. 1989). We clone 4,375 galaxies to fill the ZOA and after carrying out the cloning procedure, finally we have 47,680 galaxies in our 2MRS sample. The distribution of the galactic coordinates of galaxies in the 2MRS after filling the ZOA is shown in the right panel of Figure 1. We construct 30 jackknife samples from the 2MRS data each containing 35,000 galaxies.

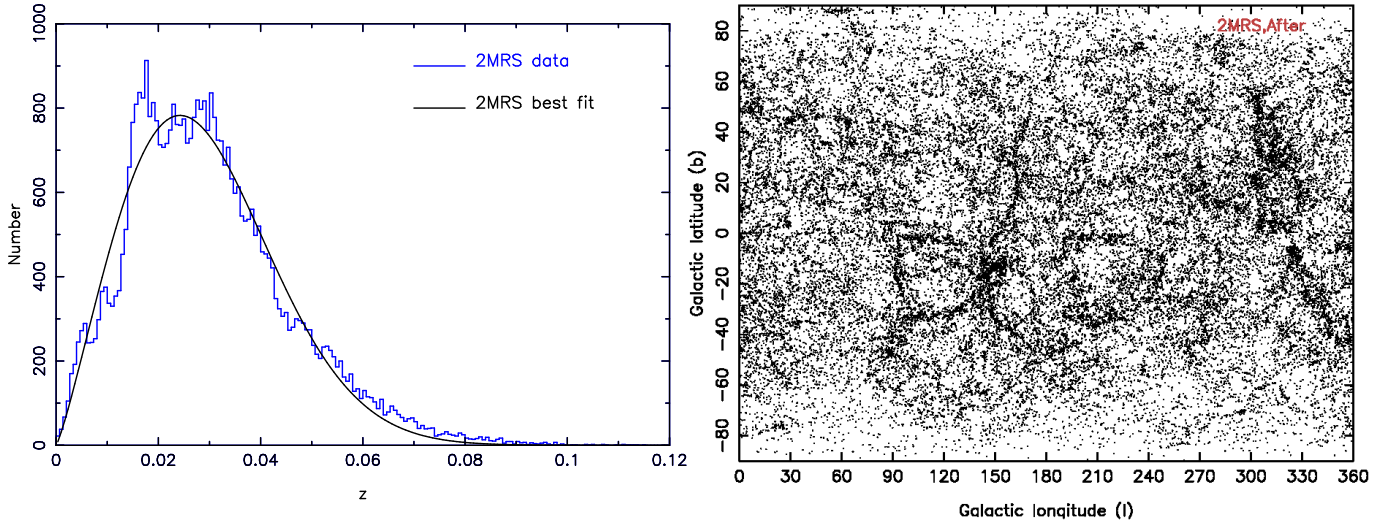


**Figure 1.** The left panel shows the redshift histogram in the 2MASS redshift survey (2MRS) along with the best fit (Equation 7) to it. The right panel shows the distribution of galactic coordinates of the 2MRS galaxies after the zone of avoidance is filled with cloned galaxies.

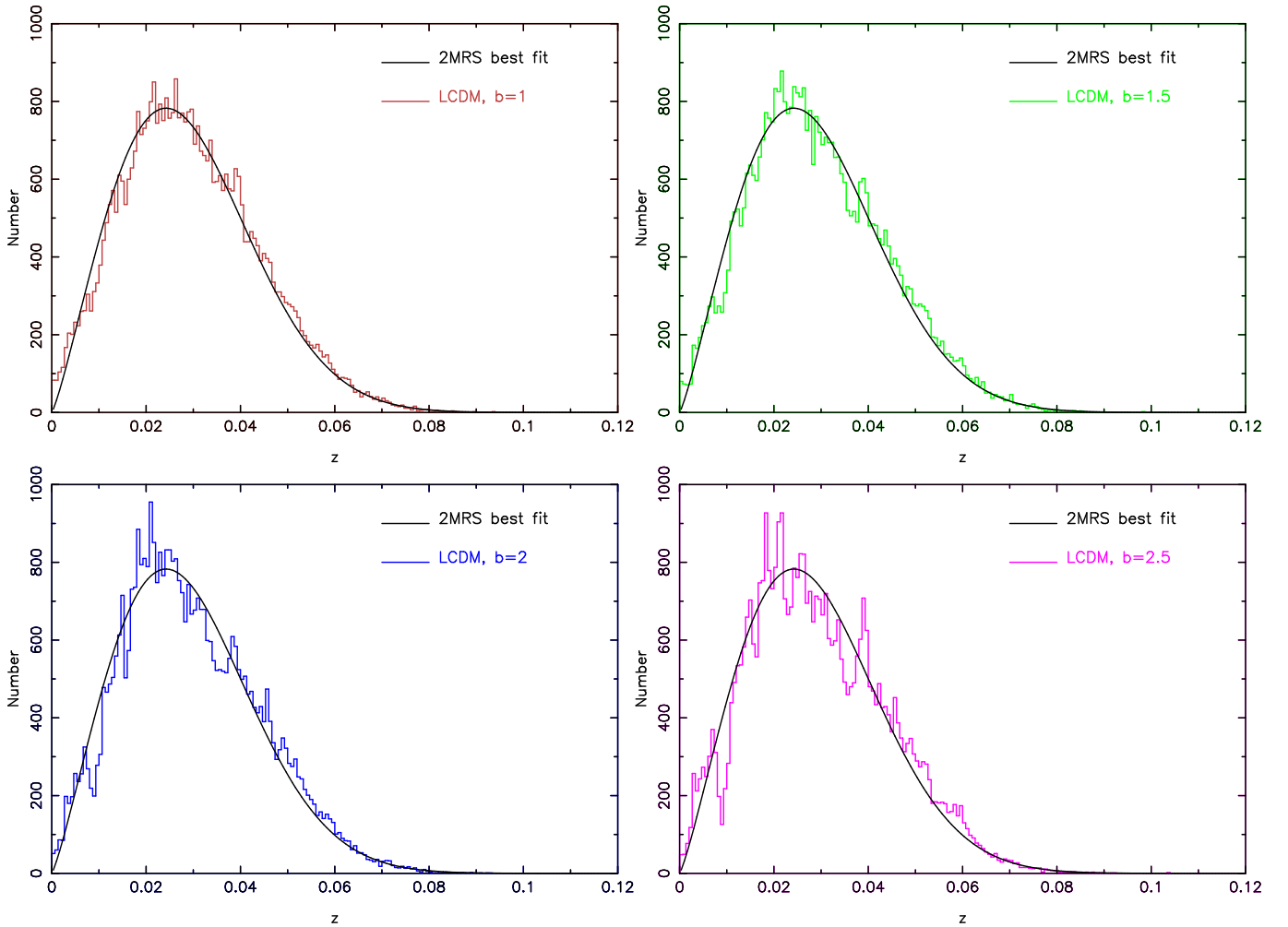


**Figure 2.** Different panels of this plot show the redshift histograms for a simulated galaxy sample with different bias values along with the best fit to the 2MRS galaxy sample. The linear bias values of the respective samples are indicated in each panel. We use the best fit (Equation 7) to the 2MRS redshift distribution to simulate the mock galaxy catalogues for unbiased and biased distributions from N-body simulation of the  $\Lambda$ CDM model.



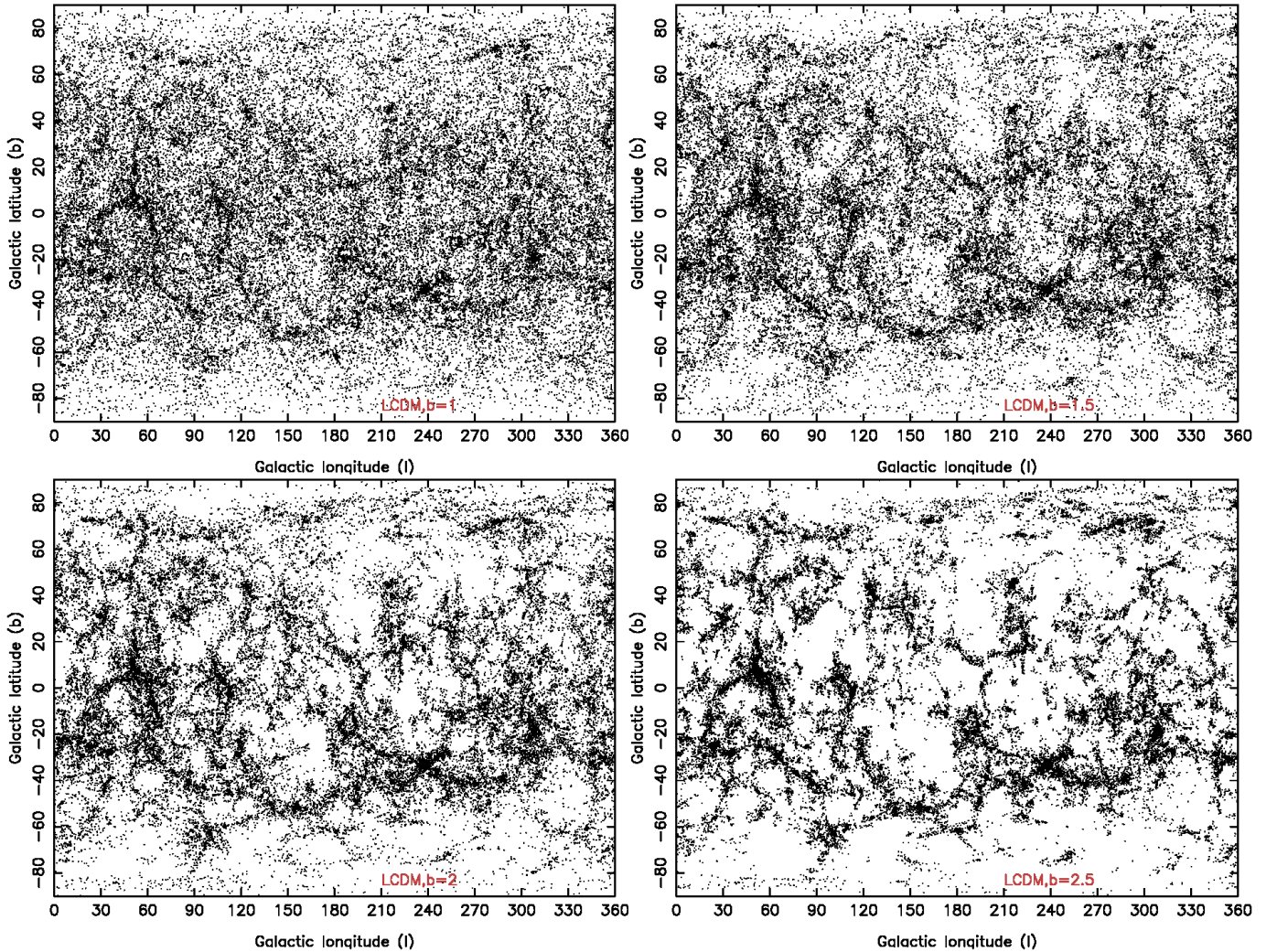


**Figure 3.** This shows the galactic coordinates in a mock 2MRS galaxy sample with different bias values as indicated in each panel.

### 3.2 MOCK CATALOGUES FROM N-BODY SIMULATION

We use a Particle-Mesh (PM) N-body code to simulate the present day distributions of dark matter in the  $\Lambda$ CDM model in a comoving volume of  $[921.6h^{-1}\text{Mpc}]^3$ . We use  $256^3$  particles on a  $512^3$  mesh and the following cosmological parameters:  $\Omega_{m0} = 0.31$ ,  $\Omega_{\Lambda0} = 0.69$ ,  $h = 0.68$ ,  $\sigma_8 = 0.81$  and  $n_s = 0.96$  (Planck Collaboration et al. 2016) are used in the simulation. In the current paradigm, the galaxies are believed to form at the peaks of the density field. We implement a simple biasing scheme (Cole, Hatton & Weinberg 1998) where the galaxies are allowed to form only in those peaks where the overdensity exceeds a certain density threshold. One can vary the threshold in this sharp cut-off biasing scheme to generate galaxy distributions with different bias values. We determine the linear bias parameter  $b$  for these samples as,

$$b = \sqrt{\frac{\xi_g(r)}{\xi_m(r)}} \quad (8)$$

where  $\xi_g(r)$  and  $\xi_m(r)$  are the two-point correlation functions for the galaxy and dark matter distribution respec-

tively. We generate the distributions for three different bias values  $b = 1.5$ ,  $b = 2$  and  $b = 2.5$ .

We construct a set of mock 2MRS catalogues from the unbiased and biased distributions. The function given in Equation 7 has the maxima at  $z = z_c(\frac{\gamma}{\alpha})^{\frac{1}{\alpha}}$ . Substituting the best fit values of the parameters  $A$ ,  $\gamma$ ,  $z_c$  and  $\alpha$ , we find that the maximum probability of finding a galaxy in the 2MRS sample is at  $z_{max} = 0.0242$ . One can then calculate the maximum probability  $P_{max}$  from Equation 7 using the values of  $z_{max}$  and the best fit parameters. To simulate the 2MRS mock catalogues from the N-body simulation and the biased distributions, we treat the particles as galaxies and place an observer at the center of the box. We map the galaxies to redshift space using their peculiar velocities. We randomly choose a galaxy within the redshift range  $0 \leq z \leq 0.12$  and calculate the probability of detecting this galaxy using Equation 7. We also randomly choose a probability value in the range  $0 \leq P(z) \leq P_{max}$ . If the calculated probability is larger than the randomly selected probability then we retain the randomly selected galaxy in our sample. This process is repeated until we have 47,680 galaxies in the mock sample. We extract 30 mock samples for each bias values. We show the all sky distribution of the

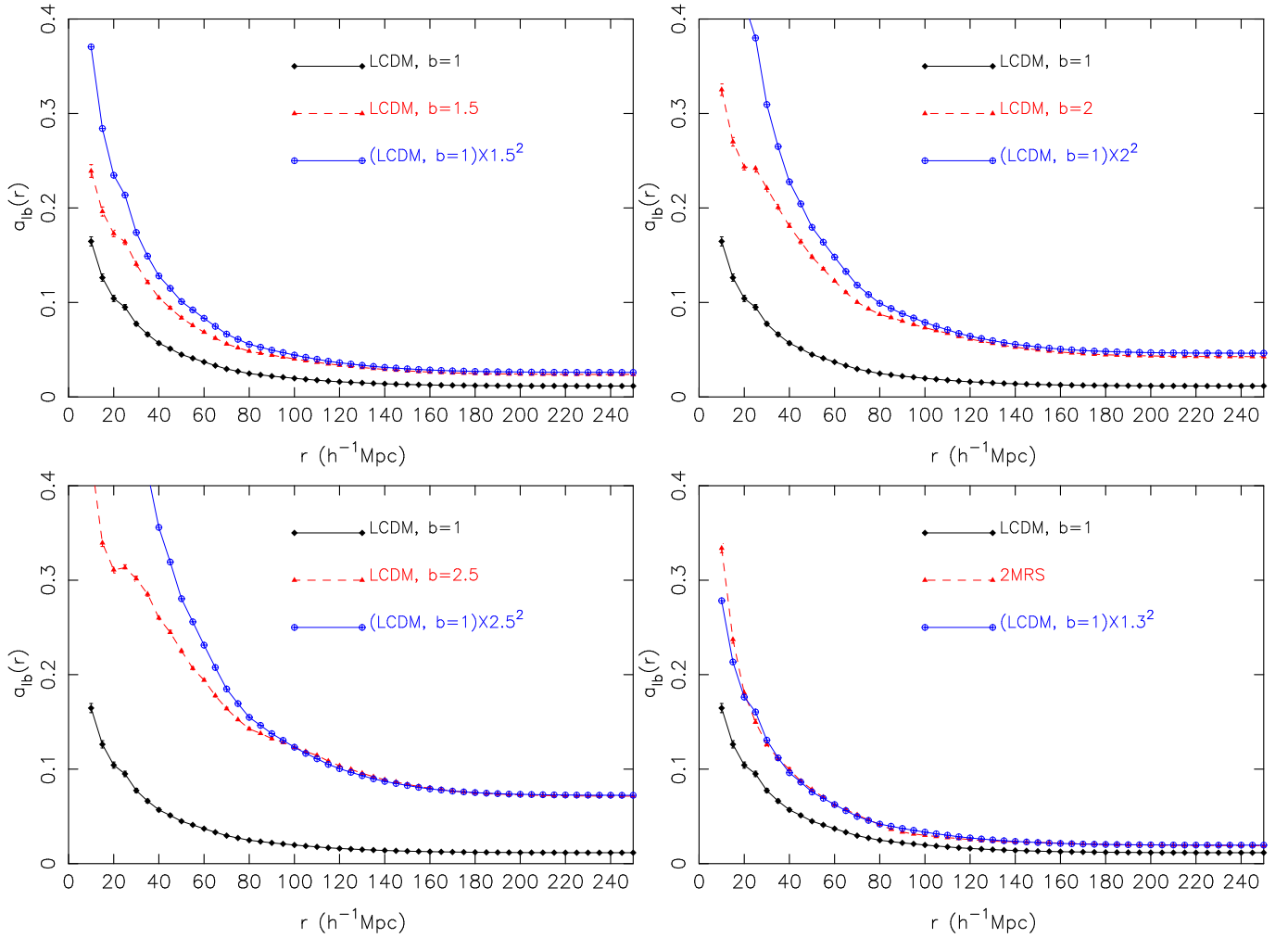


**Figure 4.** The top left, top right and bottom left panel show that the radial anisotropies in the simulated galaxy samples can be obtained by scaling the radial anisotropies in the dark matter distribution by  $b^2$  where  $b$  is the linear bias parameter of the simulated galaxy sample. The bottom right panel shows that the radial anisotropies in the 2MRS galaxy samples is well represented by the radial anisotropies expected in a galaxy distribution in  $\Lambda$ CDM model with linear bias  $b = 1.3$ . The radial anisotropies for the simulated samples shown in each panel are the mean anisotropies obtained from 30 mocks in each case. The  $1\sigma$  errorbars shown in each panel are obtained from 30 mock catalogues for the N-body simulations and 30 jackknife samples for the 2MRS data.

galactic coordinates for a mock 2MRS sample with different bias values in Figure 3.

#### 4 RESULTS AND CONCLUSIONS

In Figure 4 we compare the radial anisotropies  $a_{lb}(r)$  in the simulated mock biased galaxy samples with that from the mock samples from the dark matter distribution in the  $\Lambda$ CDM model. The top left panel, top right panel and the bottom left panel of Figure 4 show the comparisons for linear bias values  $b = 1.5$ ,  $b = 2$  and  $b = 2.5$  respectively. We see in each of these panels that scaling the radial anisotropy with  $b^2$  where  $b$  is the linear bias parameter of the simulated galaxy sample, reproduces the actual radial anisotropies observed in the respective galaxy samples on large scales. However this scaling shows a large deviation on small scales which gradually decreases and finally merges with the observed radial anisotropies in the biased samples beyond a length scale of  $90 h^{-1}$  Mpc. We do not expect the linear bi-

asing to hold on small scales. On small scales, the differences result from the non-linearities present on those scales due to the gravitational clustering. The contributions from the higher order moments of the probability distribution in Equation 3 are not negligible on smaller scales and the bias values obtained by using Equation 6 are expected to deviate from its actual value. Eventually the assumption of linear bias may prevail on some larger scale and the Equation 6 can faithfully recover the linear bias values only on a scale where the non-linearity becomes negligible. In the bottom right panel of Figure 4 we compare the radial anisotropies in the 2MRS galaxy sample with that expected from the unbiased  $\Lambda$ CDM model. Interestingly, when we scale the radial anisotropies in the unbiased  $\Lambda$ CDM model by  $1.3^2$  we find that it nicely represents the radial anisotropies observed in the 2MRS galaxy sample for nearly the entire length scales beyond  $20 h^{-1}$  Mpc. This indicates that the non-linearity becomes less important in the 2MRS galaxy sample beyond a length scale of  $20 h^{-1}$  Mpc. It is also interesting to note that though the radial anisotropy in all the biased galaxy distri-

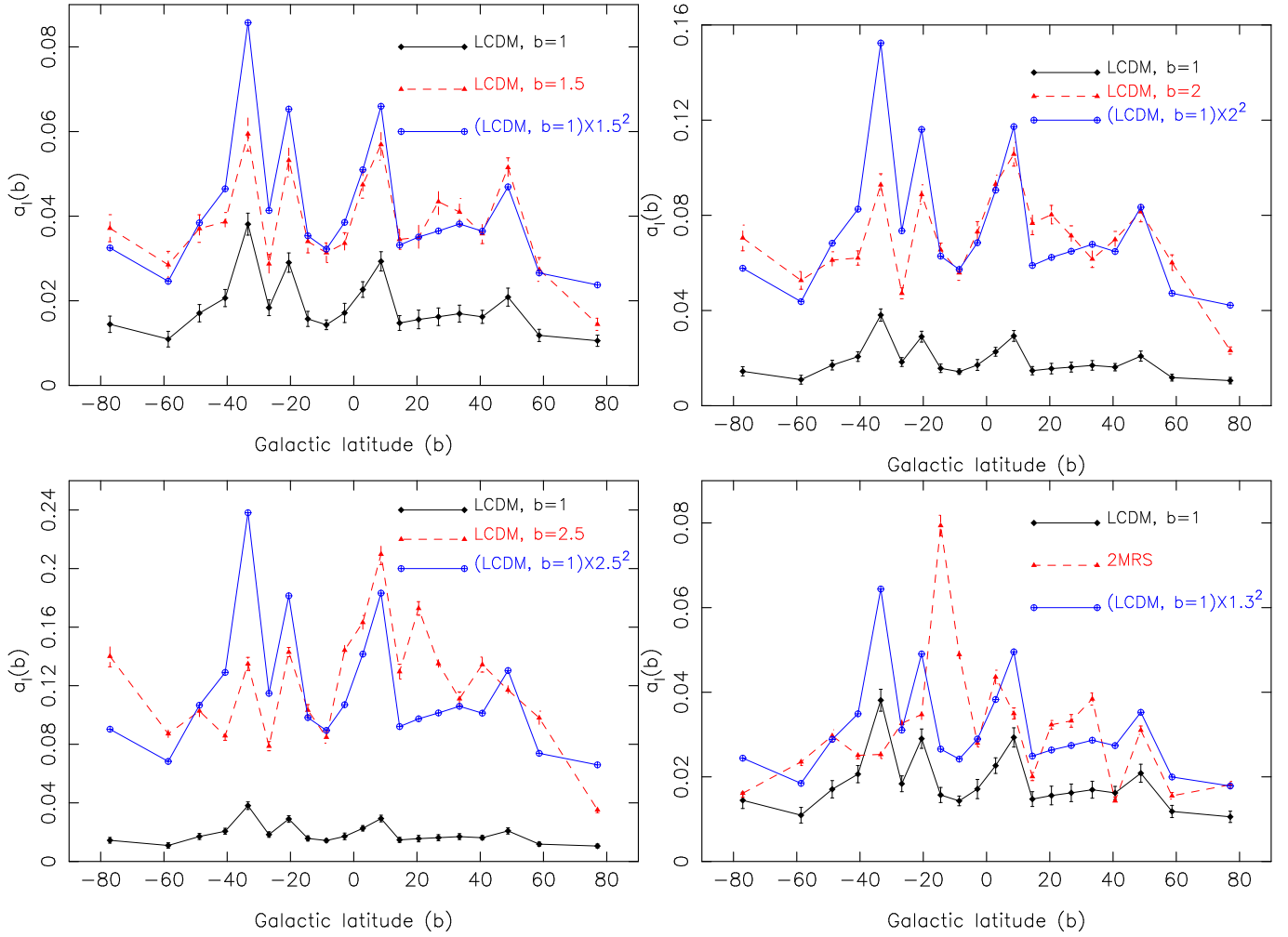


**Figure 5.** Same as Figure 4 but for polar anisotropies.

butions decreases with increasing length scales, they reach a plateau at different length scales. We note that for  $b = 1$ ,  $b = 1.5$ ,  $b = 2$  and  $b = 2.5$  the plateaus are reached at  $90 h^{-1}$  Mpc,  $130 h^{-1}$  Mpc,  $150 h^{-1}$  Mpc and  $170 h^{-1}$  Mpc respectively. This indicates that the signatures of anisotropy may persist up to different length scales depending on the bias of the galaxy distribution.

Our scheme maintains equal area for all the pixels by uniformly binning  $\cos\theta$  and  $\phi$ . This causes the shapes of the pixels to vary across different parts of the sky. These variations may contribute to the anisotropies measured in our scheme. To assess this we carry out some tests with HEALPix (Górski et al. 1999, 2005) which uses equal area and nearly same shape for all the pixels. We calculate the radial anisotropy in the same datasets using NSide = 8 in HEALPix which provides a total 768 pixels on the sky. It may be noted that we use  $m_b = 20$  and  $m_l = 40$  in our scheme which results into a total 800 pixels. We find that HEALPix pixelization gives exactly the same radial anisotropy as measured in our scheme (Pandey 2017).

We compare the polar and azimuthal anisotropies in the biased and unbiased samples in the top left, top right and bottom left panels of Figure 5 and Figure 6 respectively. We notice that a scaling similar to Figure 4 also applies

here despite the fact that a smaller number galaxies are used to compute the anisotropies at each  $b$  and  $l$ . It may be noted that the peaks and troughs in the polar and azimuthal anisotropy curves for the simulated samples appear nearly at the same  $l$  and  $b$  values as the biased distributions are produced from the same unbiased distribution. But if we compare these results with that from a galaxy distribution, we do not expect this to happen as they represent two different statistical realizations of the density field. We find that the Equation 6 can be also used effectively with polar and azimuthal anisotropies to recover the linear bias parameter of the biased galaxy samples (Table 1). We consider the polar and azimuthal anisotropies estimated from 30 samples in each case to measure the linear bias values using Equation 6 respectively at each latitude ( $b$ ) and longitude ( $l$ ). We estimate the average linear bias values and their standard errors by combining the bias measurements over different latitudes and longitudes and list them in Table 1.

In Table 1 we see that the linear bias values recovered for the simulated galaxy samples are quite close to their actual bias values. When we apply the same method to estimate the linear bias of the 2MRS galaxy sample, we get  $b = 1.31$  from polar anisotropy and  $b = 1.29$  from azimuthal anisotropy. It is interesting to note that we get

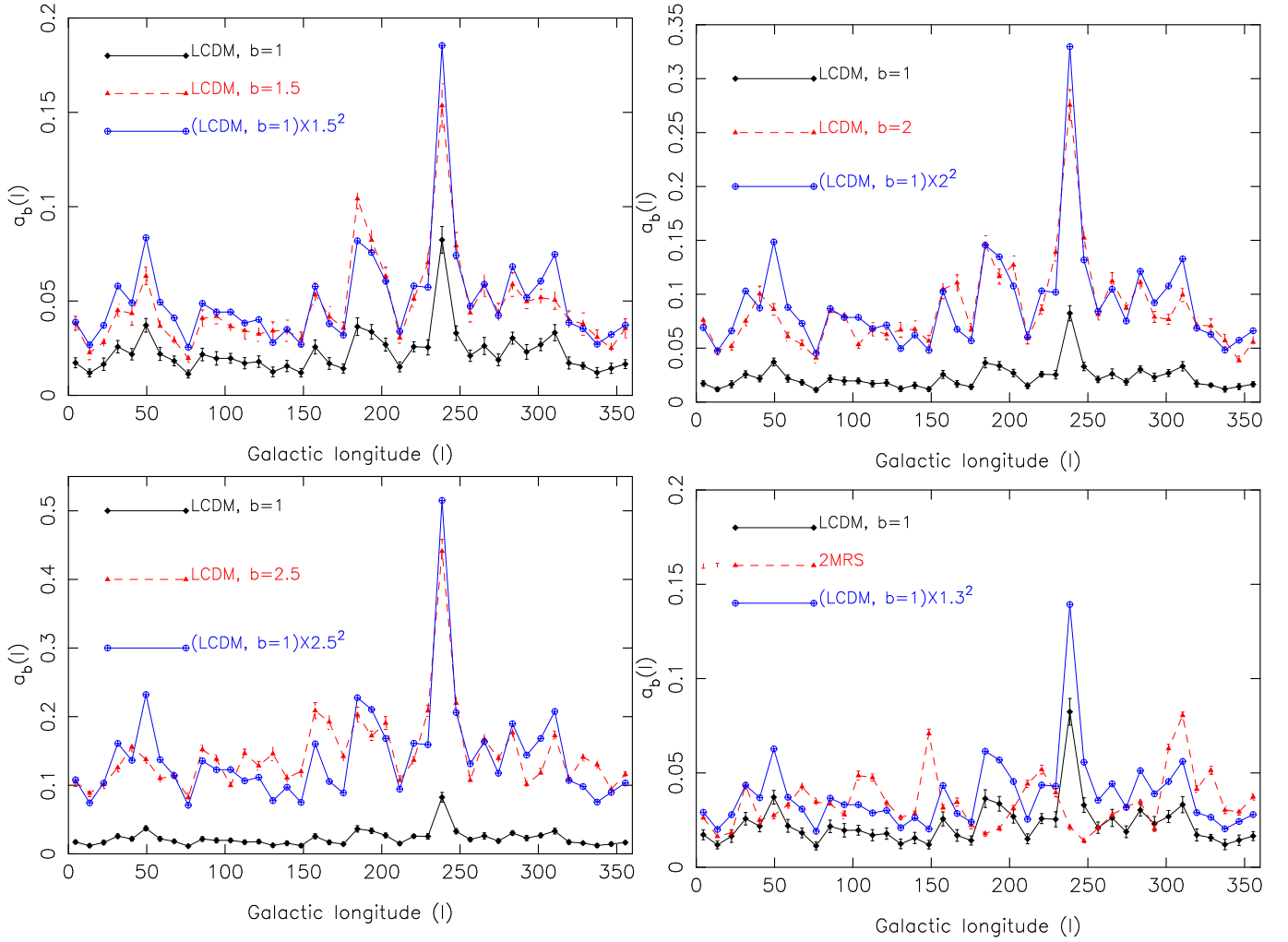


**Figure 6.** Same as Figure 4 but for azimuthal anisotropies.

**Table 1.** This shows the linear bias values estimated from the polar and azimuthal anisotropies for the simulated samples and the 2MRS sample. We calculate the linear bias values using Equation 6 but with the average polar and azimuthal anisotropies measured from the 30 samples in each case. We average the bias measurements from polar and azimuthal anisotropies over different latitudes and longitudes respectively. The errors quoted with the bias values in the table are the standard errors.

Sample	Bias from $a_l(b)$	Bias from $a_b(l)$
$\Lambda$ CDM, $b=1$	1	1
$\Lambda$ CDM, $b=1.5$	$1.45 \pm 0.026$	$1.44 \pm 0.017$
$\Lambda$ CDM, $b=2$	$1.96 \pm 0.051$	$1.96 \pm 0.033$
$\Lambda$ CDM, $b=2.5$	$2.57 \pm 0.089$	$2.6 \pm 0.053$
2MRS	$1.31 \pm 0.067$	$1.29 \pm 0.055$

nearly the same bias value  $b \sim 1.3$  from radial, polar and azimuthal anisotropies. One can also determine the relative bias parameter between any two galaxy distributions using the same method.

We also test the applicability of this method to mock samples where the radial selection function is uniform. We randomly extract  $10^5$  particles from 10 spherical regions of radius  $200 h^{-1}$  Mpc from each of the biased and unbiased distributions and repeated the analysis. We find that one can recover the linear bias of the simulated galaxy samples following the same method presented in this work. This sug-

gests that the same method can be applied to determine the linear bias parameter of the volume limited sample from different galaxy surveys.

It may be noted that the computation of the two-point correlation function and power spectrum scales as  $O(N^2)$  where  $N$  is the number of galaxies in the sample. So the computational requirements scales very fast with the size of the sample. Use of tree algorithms or FFT can reduce this scaling to  $O(N \log N)$  (Szapudi & Szalay 1998; Pen 2003; Szapudi et al. 2005). Interestingly the method presented in this work requires a scaling of only  $O(N)$  and hence it is



computationally least expensive among all the other existing methods for the determination of linear bias.

We finally note that a combined study of the radial, polar and azimuthal anisotropies in the galaxy distribution provides a powerful new alternative to measure the linear bias parameter from galaxy distributions.

## 5 ACKNOWLEDGEMENT

The author thanks an anonymous reviewer for the valuable comments and suggestions. The author would like to thank the 2MRS team for making the data public. The author acknowledges financial support from the SERB, DST, Government of India through the project EMR/2015/001037. I would also like to acknowledge IUCAA, Pune and CTS, IIT, Kharagpur for providing support through associateship and visitors programme respectively.

## REFERENCES

- Alonso, D., Salvador, A. I., Sánchez, F. J., et al. 2015, MNRAS, 449, 670
- Blake, C., & Wall, J. 2002, Nature, 416, 150
- Briggs, M. S., Paciesas, W. S., Pendleton, G. N., et al. 1996, ApJ, 459, 40
- Cole, S., Hatton, S., Weinberg, D. H., & Frenk, C. S. 1998, MNRAS, 300, 945
- Colles, M. et al. (for 2dFGRS team) 2001, MNRAS, 328, 1039
- Dekel A., Rees M. J. 1987, Nature, 326, 455
- Erdoğdu, P., Lahav, O., Huchra, J. P., et al. 2006, MNRAS, 373, 45
- Erdoğdu, P., Huchra, J. P., Lahav, O., et al. 2006, MNRAS, 368, 1515
- Feldman, H. A., Frieman, J. A., Fry, J. N., & Scoccimarro, R. 2001, Physical Review Letters, 86, 1434
- Gaztañaga, E., Norberg, P., Baugh, C. M., & Croton, D. J. 2005, MNRAS, 364, 620
- Gupta, S., & Saini, T. D. 2010, MNRAS, 407, 651
- Fixsen, D. J., Cheng, E. S., Gales, J. M., et al. 1996, ApJ, 473, 576
- Gorski, K. M., Wandelt, B. D., Hansen, F. K., Hivon, E., & Banday, A. J. 1999, arXiv:astro-ph/9905275
- Górski, K. M., Hivon, E., Banday, A. J., et al. 2005, ApJ, 622, 759
- Hamilton, A. J. S. 1992, ApJ Letters, 385, L5
- Hawkins, E., et al. 2003, MNRAS, 346, 78
- Hazra, D. K., & Shafieloo, A. 2015, JCAP, 11, 012
- Huchra, J. P., Macri, L. M., Masters, K. L., et al. 2012, ApJS, 199, 26
- Kaiser, N. 1984, ApJ Letters, 284, L9
- Kaiser, N. 1987, MNRAS, 227, 1
- Lin, H.-N., Wang, S., Chang, Z., & Li, X. 2016, MNRAS, 456, 1881
- Lynden-Bell, D., Lahav, O., & Burstein, D. 1989, MNRAS, 241, 325
- Meegan, C. A., Fishman, G. J., Wilson, R. B., et al. 1992, Nature, 355, 143
- Marinoni, C., Bel, J., & Buzzi, A. 2012, JCAP, 10, 036
- Norberg, P., et al. 2001, MNRAS, 328, 64
- Pandey, B. 2016, MNRAS, 462, 1630
- Pandey, B. 2016, MNRAS, 463, 4239
- Pandey, B. 2017, Accepted in MNRAS, arXiv:1703.01184
- Peebles, P. J. E. 1980, The large scale structure of the Universe. Princeton, N.J., Princeton University Press, 1980, 435 p.,

Pen, U.-L. 2003, MNRAS, 346, 619

Planck Collaboration, Ade, P. A. R., Aghanim, N., et al. 2016, A&A, 594, A13

Scharf, C. A., Jahoda, K., Treyer, M., et al. 2000, ApJ, 544, 49

Shannon, C. E. 1948, Bell System Technical Journal, 27, 379-423, 623-656

Smoot, G. F., Bennett, C. L., Kogut, A., et al. 1992, ApJ Letters, 396, L1

Szapudi, I., & Szalay, A. S. 1998, ApJ Letters, 494, L41

Szapudi, I., Pan, J., Prunet, S., & Budavári, T. 2005, ApJ Letters, 631, L1

Tegmark, M., et al. 2004, ApJ, 606, 702

Verde, L., Heavens, A. F., Percival, W. J., et al. 2002, MNRAS, 335, 432

Wilson, R. W., & Penzias, A. A. 1967, Science, 156, 1100

Wu, K. K. S., Lahav, O., & Rees, M. J. 1999, Nature, 397, 225

York, D. G., et al. 2000, AJ, 120, 1579

Zehavi, I., Zheng, Z., Weinberg, D. H., et al. 2011, ApJ, 736, 59

This paper has been typeset from a  $\text{\TeX}/\text{\LaTeX}$  file prepared by the author.